

# Dual-energy cardiac computed tomography for differentiating cardiac myxoma from thrombus

Yoo Jin Hong · Jin Hur · Young Jin Kim ·  
Hye-Jeong Lee · Sae Rom Hong · Young Joo Suh ·  
Hee Yeong Kim · Ji Won Lee · Byoung Wook Choi

Received: 9 June 2014 / Accepted: 3 July 2014 / Published online: 11 July 2014  
© Springer Science+Business Media Dordrecht 2014

**Abstract** Although intra-cardiac masses are rare, diagnosis and refined characterization of these masses are important because of the different therapeutic strategies used to treat these lesions. The purpose of this study was to evaluate the diagnostic value of dual-energy cardiac computed tomography (CCT) for differentiating cardiac myxomas from thrombi. Our institutional review board approved this study, and patients provided informed consent. We prospectively enrolled 37 patients who had an intra-cardiac mass on echocardiography or computed tomography (CT). All patients underwent dual-energy CCT. For quantitative analysis, the CT attenuation density and iodine concentration of the intra-cardiac mass were measured on CT images. The Mann–Whitney test was used to evaluate differences in the mean CT attenuation density and the mean iodine concentrations between the cardiac myxoma and thrombus groups. Pathological results or follow-up with echocardiography was used to make the final diagnosis. There were a total of 17 cardiac myxomas and 20 thrombi. On CT, the mean CT numbers were not significantly different between cardiac myxomas and cardiac thrombi ( $91.7 \pm 11.6$  HU vs.  $85.2 \pm 10.9$  HU, respectively,  $P = 0.241$ ), whereas, the mean iodine concentration (mg/ml)

was significantly different between cardiac myxomas and cardiac thrombi ( $3.53 \pm 0.72$  vs.  $1.37 \pm 0.31$ , respectively,  $P < 0.001$ ). Dual-energy CCT using a quantitative analytic methodology can be used to differentiate between cardiac myxomas and thrombi.

**Keywords** Dual-energy computed tomography (DECT) · Cardiac myxoma · Cardiac thrombus · Differential diagnosis

## Abbreviations

CCT	Cardiac computed tomography
CMR	Cardiovascular magnetic resonance
CT	Computed tomography
DECT	Dual-energy computed tomography
GSI	Gemstone spectral imaging
LA	Left atrium
LAA	Left atrial appendage
LV	Left ventricle
RA	Right atrium
ROI	Region of interest
RV	Right ventricle

Y. J. Hong · J. Hur (✉) · Y. J. Kim · H.-J. Lee ·  
S. R. Hong · Y. J. Suh · B. W. Choi  
Department of Radiology and Research Institute of Radiological  
Science, Severance Hospital, Yonsei University College of  
Medicine, 50 Yonsei-ro, Seodaemun-gu, Seoul 120-752, Korea  
e-mail: khuhz@yuhs.ac

H. Y. Kim  
Department of Radiology, Kangwon National University  
Hospital, Chuncheon, Korea

J. W. Lee  
Department of Radiology, Pusan National University Hospital,  
Pusan, Korea

## Introduction

Although intra-cardiac masses are rare, diagnosis and refined characterization of these masses are important due to the high morbidity and mortality associated with the functional consequences of such tumors and the potential for arrhythmia or emboli [1–3]. It is clinically important to differentiate cardiac tumors from cardiac tumor-like lesions, such as thrombi, because of the different therapeutic strategies used to treat these lesions [4–6]. Our hypothesis is that dual-energy

computed tomography (DECT) offers a new way to differentiate between cardiac tumors and thrombi.

Imaging plays a key role in establishing the diagnosis of patients with cardiac myxomas and thrombi because the clinical presentation is often diverse and nonspecific. Magnetic resonance imaging (MRI) is presently the modality of choice to evaluate cardiac tumors. Optimal tumor characterization may be achieved with cardiac MRI, which provides an unrestricted field-of-view and superior soft tissue depiction without ionizing radiation [7, 8]. Multi-detector computed tomography (MDCT) is increasingly being utilized for cardiac imaging [3]. However, CT lacks the superior soft-tissue contrast abilities of MRI and is therefore not suitable for differentiating between cardiac myxomas and thrombi [9]. DECT is a technological advancement in imaging, allowing greater material differentiation by using two data sets from different X-ray spectra. Obtaining CT data at different photon energies allows for the detection of differences in material composition based on differences in photon absorption rates at high and low kVp settings [10]. Using this technique, it is possible to differentiate iodine from other materials using the material decomposition method [10–12]. Because most thrombi do not show enhancement, but tumors usually do show enhancement, we hypothesized that DECT would be valuable for differentiating cardiac myxomas from thrombi. The purpose of this study was to evaluate the diagnostic value of dual-energy cardiac computed tomography (CCT) for differentiating cardiac myxomas from thrombi.

## Materials and methods

### Patient population

This single-center prospective study was approved by our institutional review board, and informed consent was obtained from all patients. From June 2011 to July 2012, a total of 55 consecutive patients who had a suspicious intracardiac mass on echocardiography or conventional CT were prospectively enrolled to undergo dual-energy CCT.

The exclusion criteria were pericardial or myocardial mass ( $n = 5$ ), inconclusive final results ( $n = 2$ ), contrast agent allergy ( $n = 2$ ), renal dysfunction ( $n = 1$ ), and refusal to provide written informed consent ( $n = 8$ ). The final group of 37 patients consisted of 25 males and 12 females (mean age, 60.9 years; range 35–88 years). The patients' baseline clinical history characteristics, including systemic hypertension, hyperlipidemia, diabetes mellitus, smoking habits, history of cardiovascular disease, cerebral vascular disease, and other heart disease were recorded from medical records and routine laboratory data. The final diagnoses were based on either pathological results ( $n = 19$ ; 17 cardiac myxomas

and 2 thrombi) or a follow-up examination including echocardiography, or MRI after anticoagulant treatment without other treatment ( $n = 18$ , cardiac thrombi).

### Dual-energy cardiac computed tomography examination (CCT)

DECT scans were performed with a 64-row multidetector CT scanner (Discovery CT750 HD; GE Healthcare, India) in the cranio-caudal direction during a single breath-hold. Scanning was performed with the second injection of contrast agent, 180 s after the end of the first bolus injection of contrast agent. The double injection protocol was based on our previous studies [13, 14].

No beta-blockers were used to regulate the heart rate, because CT was performed to evaluate the intracardiac structure and not the coronary arteries. The mean heart rate was  $64.9 \pm 8$  beats per min (range 47–88 beats/min) during the CT examination.

For the first bolus injection, 50 ml of the nonionic contrast agent, iopamidol (370 mg of iodine per milliliter, Iopamiro; Bracco, Milan, Italy), was administered using a power injector (Envision CT, Medrad, Indianola, PA, USA) at a rate of 5 ml/s via an 18-gauge needle placed into the right antecubital vein. Following contrast agent administration, 50 ml of saline was administered at a flow rate of 5 ml/s through the same venous access. A region of interest (ROI) was plotted inside the ascending aorta and a bolus geometry curve was acquired. Curve diagrams were analyzed immediately after acquisition, and the time to maximum enhancement was measured to determine the optimal scan delay.

Using the gemstone spectral imaging (GSI) mode (DECT mode), the scan was started at 180 s, after the end of the first bolus injection. The second bolus, composed of 70 ml of the nonionic contrast agent, iopamidol (370 mg of iodine per milliliter, Iopamiro; Bracco, Milan, Italy), followed by a 50-ml contrast-saline mixture at a ratio of 30:70, was administered intravenously at a rate of 5 ml/s using a power injector (Envision CT, Medrad). The scan parameters were as follows: detector collimation,  $64 \times 0.625$  mm; gantry rotation time, 0.5 s; tube voltage, 140 and 80 kV; tube current, 630 mAs; and pitch, 1.375:1. All images were reconstructed with a slice thickness of 0.625 mm and a detail reconstruction kernel, and evaluated on an off-line workstation (GE workstation, Volumeshare 4.4.5, GE Healthcare, Milwaukee, WI, USA).

### Image analysis

CT data were assessed by two experienced radiologists with 3 and 7 years of experience in cardiac CT, respectively, who were blinded to patient identities and clinical histories. All scans were processed and read on a dedicated workstation

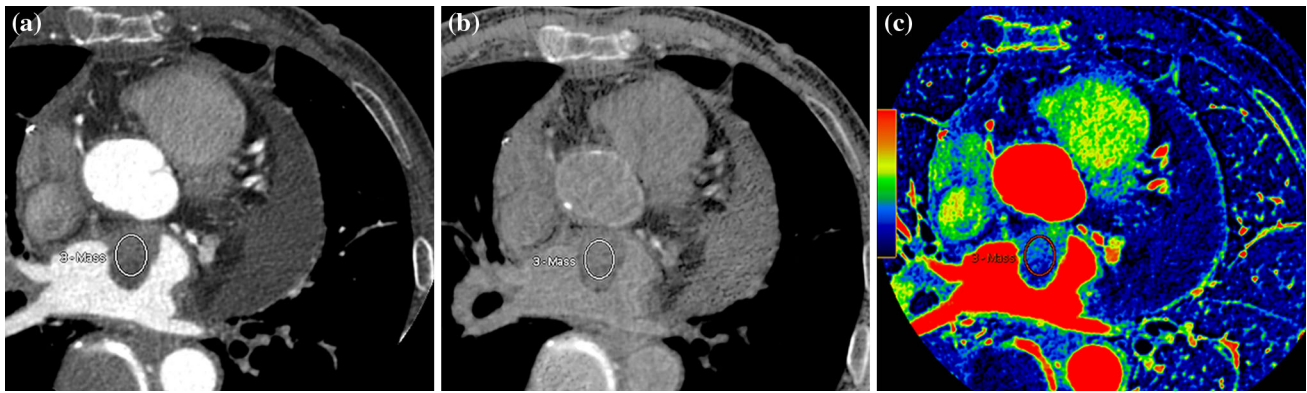


**Fig. 1** Example image set from a patient with a cardiac tumor. Three modes of images obtained by dual-energy CT data, monochromatic 70 keV image representing post-contrast CT image (a), MSI image

representing pre-contrast CT image (b), and iodine (water) image demonstrating identical level of the cardiac tumor were displayed on the workstation (c)

equipped with dual-energy post-processing software (GE workstation, Volumeshare 4.4.5, GE Healthcare).

Two investigators recorded the size and location of the intra-cardiac masses; left atrium (LA), left ventricle (LV), right atrium (RA), or right ventricle (RV). Measurement of mass size was based on the longest long and short axes. The two investigators evaluated the morphological appearance and differences in assessment were resolved by consensus. Each mass was characterized in terms of its shape (round, oval, lobular, irregular), and internal characteristics (calcification, necrosis, or cystic).

For quantitative analysis, the two radiologists measured the mean CT attenuation density of masses at two different slices selected independently by the two reviewers in Hounsfield unit (HU) among the monochromatic 70 keV images in order to approximate those of conventional 120 kV images. Reviewers selected the slice that showed the largest part of the mass and the mean HU of the mass was used for analysis. On post-contrast CT images, a circular ROI was drawn within the mass to be as large of an area as possible. The reviewers also measured the mean CT attenuation value of the mass in HU with material-suppressed iodine (MSI) images provided by the workstation. The MSI images were used to measure the HUs that were used to approximate those of non-enhanced 120 kV images to calculate the mean iodine-related HU (IHU) of the masses. The mean IHU was calculated as follows:  $IHU = \text{post enhanced HU} - \text{non-enhanced HU}$ .

The reviewers also measured the iodine concentration of the masses with the iodine (water) images provided by the workstation. The two radiologists independently measured iodine concentrations (mg/ml) on the same slice with which HU was measured; averaged values were used for analysis. The three modes of images, monochromatic 70 keV images representing post-contrast CT images, MSI images representing pre-contrast CT images, and iodine (water) images could be displayed on the workstation, side by side at the same time, linked together, therefore demonstrating an

identical level of the intra-cardiac mass for each mode (Fig. 1). On the workstation, the displayed iodine (water) image provided the quantitative value of iodine (See online Appendix for fundamental equations).

### Statistical analysis

Categorical baseline characteristics were expressed as numbers and percentages, and were compared between the cardiac myxoma and thrombus groups using the Fisher's exact test. Continuous variables are expressed as means and standard deviations, and were compared with the Mann–Whitney test for independent samples. The Mann–Whitney test was also used to evaluate differences in the mean CT attenuation values of intra-cardiac masses, iodine-related HU, and mean iodine concentrations between the cardiac myxoma and thrombus groups. We constructed receiver operating characteristics ROC curves using the iodine concentration, and determined the best cut-off value to differentiate between cardiac myxomas and thrombi. ROC curves were used to compare the performance of dual-energy CCT with that of contrast-enhanced CT for the differentiation of cardiac myxoma and thrombus. Intraclass correlation coefficients (ICC) were used to evaluate inter-observer agreement for the mean CT number and iodine concentration values measured by the two radiologists. *P* values < 0.05 were considered statistically significant. All statistical analyses were performed with statistical software (SPSS, version 18.0, SPSS, Chicago, IL, USA; and MedCalc, version 9.5, MedCalc, Mariakerke, Belgium).

### Results

The demographics and baseline clinical characteristics of the 37 patients are summarized in Table 1. Except for size,

**Table 1** Demographic and baseline characteristics of the 37 patients [n (%)]

	Cardiac myxomas (n = 17)	Thrombi (n = 20)	P values
Male	13 (76.5 %)	12 (60 %)	0.479
Age* (years)	59.3 ± 13.1	62.2 ± 13.4	0.493
Size* (mm)	29.4 ± 13.9	21.3 ± 9.04	0.048 <sup>  </sup>
Location			0.747
Left atrium (LA)	11 (64.7 %)	15 (75 %)	
Left ventricle (LV)	0	2(10)	
Right atrium (RA)	6 (35.3 %)	3 (15 %)	
Right ventricle (RV)	0	0	
Morphological appearance			
Shape			0.014 <sup>  </sup>
Round	2 (11.7 %)	8 (40 %)	
Oval	4 (23.5 %)	10 (50 %)	
Lobular	5 (29.4 %)	2 (10 %)	
Irregular	6 (35.4 %)	0	
Internal characteristic			0.401
Calcification	2 (11.7 %)	0	
Cystic/necrosis	2 (11.7 %)	0	
Mean ejection fraction	62.3 ± 4.65	56.7 ± 14.1	0.227
Past history			
Atrial fibrillation	0	14 (70 %)	<0.001 <sup>  </sup>
Hypertension	7 (41.2 %)	9 (45 %)	0.917
Diabetes mellitus	3 (17.6 %)	4 (20 %)	0.813
Smoking	5 (29.4 %)	9 (45 %)	0.525
Hyperlipidemia	1 (5.8 %)	2 (10 %)	0.890
Prior CVA/TIA <sup>†</sup>	3 (17.6 %)	8 (40 %)	0.261
Heart disease <sup>‡</sup>	2 (11.7 %)	10 (50 %)	0.033 <sup>‡</sup>
Cancer <sup>§</sup>	2 (11.7 %)	1 (5 %)	0.888
Central venous catheter	6 (35.3 %)	3 (15 %)	0.293

<sup>†</sup> CVA cerebrovascular accident, TIA transient ischemic attack

<sup>||</sup>  $P < 0.05$ , statistically significant

\* Mean ± SD

<sup>‡</sup> Heart disease includes valvular heart disease and myocardial infarction

<sup>§</sup> Cancer includes organs other than heart

shape of mass, atrial fibrillation and heart disease, the clinical characteristics of patients with tumors and those with thrombi were not significantly different. Patients with thrombi had a higher incidence of atrial fibrillation and heart disease (valvular heart disease and myocardial infarction). Cardiac thrombi had more oval or round shapes than tumors, whereas tumors had more irregular shape than

thrombi. The mean diameter of cardiac myxomas was 29.4 mm, while that of cardiac thrombi was 21.3 mm, a statistically significant difference ( $P = 0.048$ ).

Among the 37 intra-cardiac masses, 17 cases (45.9 %) were cardiac myxomas and 20 (54.1 %) were cardiac thrombi. All cardiac myxomas were confirmed by surgical excision. Two thrombi underwent surgery because they were large masses at LA and the other thrombi disappeared as a result of anticoagulation therapy, which was considered proof of diagnosis.

The mean attenuation values of cardiac myxomas and cardiac thrombi measured in HU on post-contrast CT images were not significantly different ( $91.7 \pm 11.6$  HU vs.  $85.2 \pm 10.9$  HU, respectively,  $P = 0.241$ ). However, the iodine-related HU (iodine-enhanced HU–non-enhanced HU) of cardiac myxomas and thrombi were significantly different ( $56.6 \pm 8.9$  HU vs.  $26.5 \pm 7.4$  HU, respectively,  $P < 0.001$ ) (Table 2).

On iodine maps [iodine (water) images], the mean iodine concentration (mg/ml) was significantly different for cardiac myxomas versus cardiac thrombi:  $3.53 \pm 0.72$  for cardiac myxomas versus  $1.37 \pm 0.31$  for cardiac thrombi ( $p < 0.001$ ) (Table 2; Figs. 2, 3).

When we used iodine concentrations and HU for differentiating cardiac myxomas from thrombi, the areas under the ROC curve (AUC) were 0.997 (95 % CI 0.899, 1.000) and 0.613 (95 % CI 0.439, 0.768), respectively. There was a statistically significant difference in AUC in the differentiation between cardiac myxomas and thrombi ( $P = 0.0001$ ) (Fig. 4). Using the cut-off value of 2.37 mg/ml, the sensitivity, specificity, and area under the ROC curve (AUC) for diagnosing cardiac masses were 94, 100, and 0.997 % (95 % CI 0.899, 1.000), respectively.

There was good inter-observer agreement between the two radiologists regarding the mean HU and iodine concentrations of cardiac myxomas and thrombi (ICC = 0.753 and 0.794, respectively).

**Table 2** Quantitative analysis of dual-energy CT findings for cardiac myxomas and thrombi

	Cardiac myxomas (n = 17)	Thrombi (n = 20)	P value
CT attenuation value (HU)	91.7 ± 11.6	85.2 ± 10.9	0.241
Iodine-related HU*	56.6 ± 8.9	26.5 ± 7.4	<0.001 <sup>†</sup>
Iodine concentration (mg/ml)	3.53 ± 0.72	1.37 ± 0.31	<0.001 <sup>†</sup>

<sup>†</sup>  $P < 0.05$ , statistically significant

\* Iodine-related HU (IHU) was calculated as follows: IHU post-enhanced, HU–non-enhanced HU

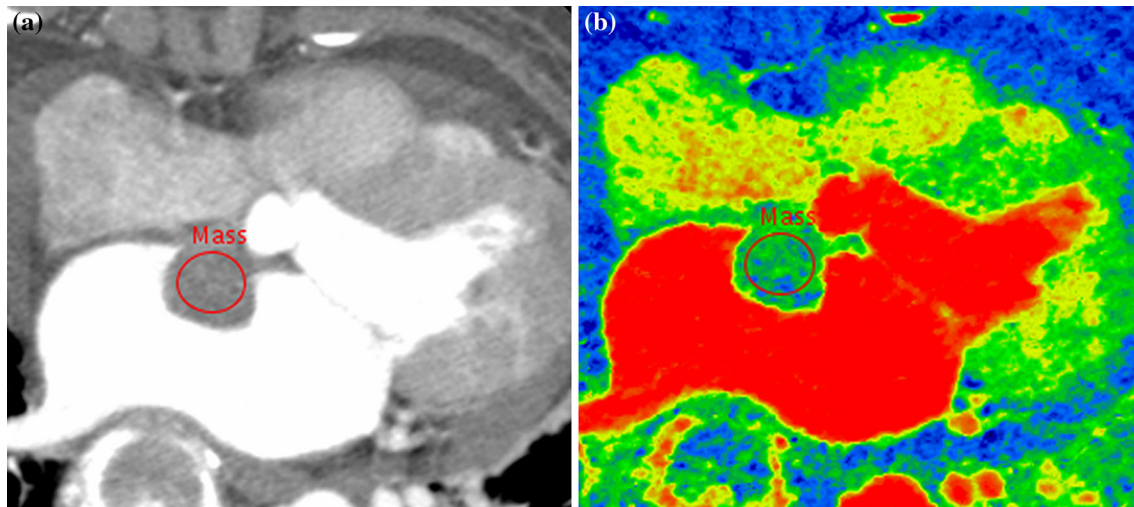


**Fig. 2** An 84-year-old female patient diagnosed with a myxoma. **a** On the enhanced CT, a  $3.2 \times 2.5$  cm well-defined low-density mass was noted in the left atrium (LA). The CT attenuation value (HU) of

the intra-cardiac mass was 82.5. **b** On the iodine (water) image, the iodine concentration of the mass within the ROI was 3.72 mg/ml

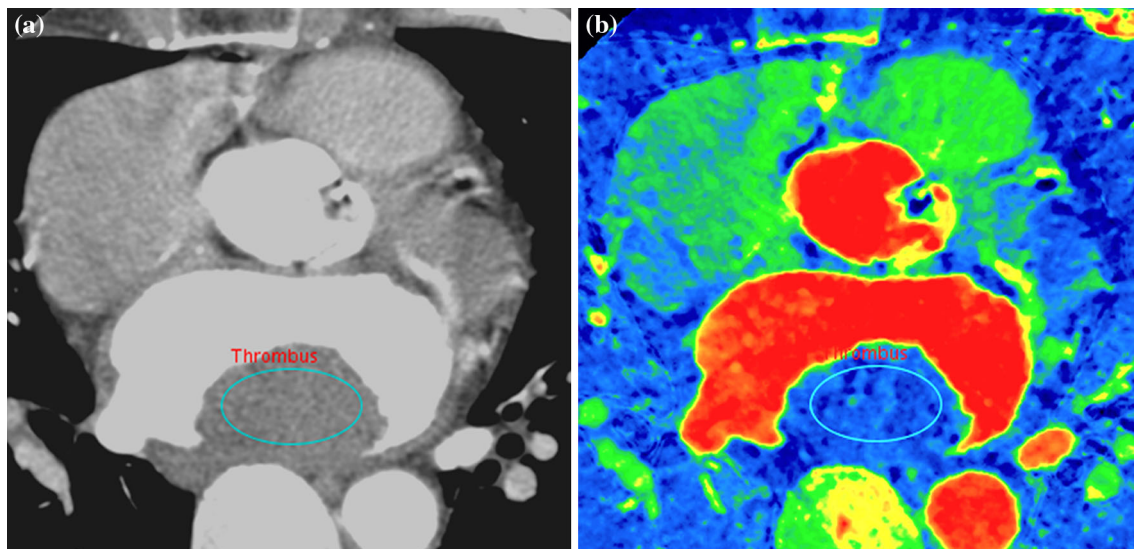


**Fig. 3** A 49-year-old male patient diagnosed with a thrombus. **a** On the enhanced CT, a  $5.8 \times 3.1$  cm well-defined low-density mass was noted in the left atrium (LA). The CT attenuation value (HU) of the

intra-cardiac mass was 79.8. **b** On the iodine (water) image, the iodine concentration within the ROI was 1.27 mg/ml

Radiation exposure was estimated from the dose-length product (DLP). The calculated mean radiation dose was 4.02 mSv (DLP range 156–317 mGy\*cm) depending on the scan range and the patient's body weight.

## Discussion

This study was designed to examine the performance of dual-energy CCT in differentiating cardiac myxomas from thrombi. Our results suggest that iodine concentration

obtained from the dual energy CT data is a feasible quantitative parameter for differentiating cardiac myxomas from thrombi. The mean attenuation value in HU measured only on post-contrast CT images failed to be a significant marker for diagnosing cardiac myxomas from thrombi, however, the iodine concentration gave statistically significant characterization of cardiac masses as myxomas or thrombi.

Accurate diagnosis of cardiac thrombi and myxomas is important because these masses provide a substrate for embolic events but are treated differently according to

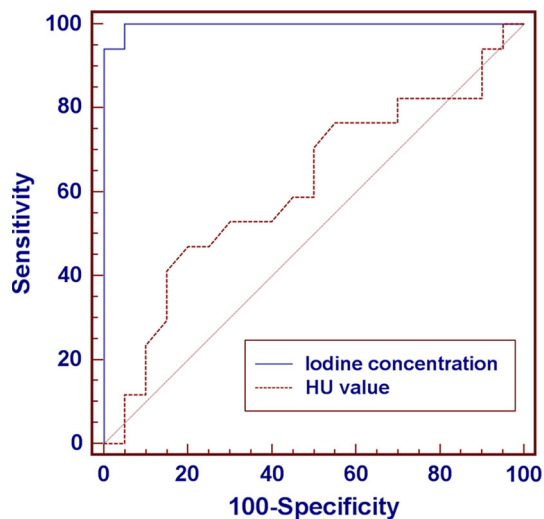


**Fig. 4** Receiver operating characteristic (ROC) curve of iodine concentration (mg/ml) and Hounsfield unit distinguishing between cardiac myxomas and thrombi. The areas under the ROC curve were 0.997 and 0.613, respectively

etiology. Surgical intervention is usually required to remove a cardiac myxoma, whereas complete resolution of a thrombus may be expected with appropriate anticoagulation therapy.

In clinical practice, echocardiography is the mainstay for tumor detection, but it has several well-described limitations, including operator dependence, a restricted field-of-view (especially in patients with a large body habitus), and occasional limited imaging of the right heart chambers. Therefore, multi-modality imaging techniques such as cardiac MRI are often used for cardiac mass evaluation. Cardiac MRI, which provides an unrestricted field-of-view and superior soft tissue depiction without ionizing radiation, is presently the modality of choice for detecting thrombi and evaluating cardiac tumors [15–18]. The advantages of cardiac MRI as compared to CT include lack of radiation exposure and avoidance of iodinated contrast media. However, cardiac MRI has several disadvantages compared to CT. The MRI examination time is much longer than CT, cardiac MRI is much more expensive than CT and MRI cannot be performed in patients with implanted metallic devices [9].

In clinical practice, CT can be used to detect cardiac masses. Cardiac myxomas and thrombi are identified from CT images based only on anatomic appearance. Although useful imaging characteristics of myxomas and thrombi can be found on CT, potential overlap in the imaging findings may result in uncertainty in the differentiation of the two disorders. Therefore, it may be challenging to differentiate a cardiac myxoma from an atrial thrombus because both can be localized at the left atrial septum and both can be irregular in shape [19, 20]. Several studies have reported that cardiac myxomas

and thrombi are difficult to differentiate based on CT attenuation values [20–21]. Scheffel et al. [20] reported that there were no significant differences in CT attenuation values between myxomas and thrombi. Consistent with these earlier studies, we also found no significant differences in CT attenuation values between cardiac myxomas and thrombi. This result suggests that the CT attenuation value is an insufficient quantitative parameter for differentiating between cardiac myxomas and thrombi. The CT number in HU merely represents different density levels of tissues and other substances. HU values can be influenced by not only iodine contrast delivered by the vascular system, but also by the presence of dense material containing blood, protein or calcification. HU values alone cannot serve as a deterministic parameter for differentiating cardiac myxomas and thrombi.

We used DECT for differentiating cardiac myxomas from thrombi. The dual-energy technique enables radiologists to differentiate contrast-enhanced structures from otherwise dense high-attenuation materials in parenchymatous organs by applying different X-ray spectra in which iodine contrast shows differing enhancement [10].

We found that dual-energy CCT based on the iodine concentrations can differentiate between cardiac myxomas and thrombi (3.53 mg/ml vs. 1.37 mg/ml, respectively,  $P < 0.001$ ) with higher diagnostic performance (AUC = 0.997, 95 % CI 0.899, 1.000) than conventional single energy cardiac CT based on the value of HU dose (AUC = 0.613, 95 % CI 0.439, 0.768). Current guidelines do not recommend cardiac CT as a first-line imaging modalities to evaluate cardiac tumor or thrombi [22, 23]. However, based on our results, we suggest that DECT can be used as a test in differentiating between cardiac tumors and thrombi in selected cases in which echocardiography or conventional contrast CT is inconclusive.

One pathologically confirmed organized thrombus, however, did show a higher iodine concentration than the mean iodine concentration of other thrombi (2.37 mg/ml). It is known that organized thrombi show contrast enhancement mainly in peripheral areas due to the fact that vascular channels are densest in the outer portions of this type of thrombus [17]. Therefore, the ability of DECT to differentiate between cardiac myxomas and organized thrombi may be limited.

Several limitations of this study should be recognized. First, our contrast injection protocol may have had a significant influence on the results. Currently, there is no standardized injection protocol for cardiac mass evaluation. Several studies have demonstrated that there is a limitation in that a scan with a single injection alone could not detect differences between tumors and thrombi [20, 21]. Therefore, the contrast injection protocol used in this study was based on our previous study, which indicated a high sensitivity and specificity for detecting and differentiating between intracardiac thrombus and spontaneous echo

contrast [13, 14]. In our previous study, we found that dual-energy CCT with a double injection protocol showed both high sensitivity and high specificity in the detection and differentiation of cardiac thrombus and circulatory stasis [14]. Because most thrombi do not show enhancement whereas tumors usually do show enhancement, we used a double injection protocol to achieve a sufficient attenuation difference between iodine-enhancing and nonenhancing lesions. In future applications of DECT in patients with cardiac tumors, the injection and scanning protocols should be considered in more detail. Second, because of the current technical limitation of the single-source CT with the dual-energy option, dual-energy CCT was performed without electrocardiography synchronization. This lack of synchronization with cardiac movements may hinder visualization of small structures inside cardiac chambers and create artifacts on images. A final limitation was radiation exposure. In our study, the calculated mean radiation dose was 4.02 mSv. The dual-energy technique utilizes the acquisition of two data sets at different energy levels, inevitably leading to greater radiation exposure to patients. Radiation dose exposure with dual energy CT is typically solved with real time dose modulation, but our CT scanner could not be equipped with current modulation via the fast kilovoltage switching method.

In conclusion, dual-energy CCT is a non-invasive modality that can differentiate between cardiac myxomas and thrombi. Therefore, we suggest that DECT is a helpful complementary tool to differentiate a myxoma from a thrombus in cases in which echocardiography or conventional contrast CT is inconclusive. Further studies are needed to ascertain whether our findings can be extended to various other histological types of cardiac tumors.

**Acknowledgments** This research was supported by Basic Science Research Program through the National Research Foundation of Korea (NRF) funded by the Ministry of Education, Science and Technology (2012-R1A1A1013152).

**Conflict of interest** None.

## Appendix

The fundamental equation for quantification of iodine.

First, the attenuation of x-rays of a single energy,  $E$ , through two known materials,  $m1$  and  $m2$  (with densities  $d1$  and  $d2$ , respectively), may be computed by:

$$p = -\ln\left(\frac{I}{I_0}\right) = d1\mu1(E) + d2\mu2(E)$$

The calculation of the monochromatic image is a linear operation performed on the material basis images and is normalized to water to ensure that the attenuation of water

is consistent with that of the polychromatic images, where water is assumed to be material  $m1$ .

$$I = I_0e^{-(\mu1(E)d1+\mu2(E)d2)}$$

where  $I_0$  is the incident radiation,  $I$  is the transmitted radiation, and  $\mu1(E)$  and  $\mu2(E)$  are the x-ray attenuation coefficients at a specific energy level  $E$ . This equation describes how the material density images are transformed to a monochromatic image at energy  $E$ .  $d1$  and  $d2$  are the material densities in milligrams per milliliter of the material density pair.

$\mu1(E)$  = Water attenuation coefficient at  $E$ .

$\mu2(E)$  = Iodine attenuation coefficient at  $E$ .

## References

- Castillo JG, Silvay G (2010) Characterization and management of cardiac tumors. *Semin Cardiothorac Vasc Anesth* 14(1):6–20
- Araoz PA, Eklund HE, Welch TJ, Breen JF (1999) CT and MR imaging of primary cardiac malignancies. *Radiographics* 19(6):1421–1434
- Tatli S, Lipton MJ (2005) CT for intracardiac thrombi and tumors. *Int J Cardiovasc Imaging* 21(1):115–131
- Doufekias E, Segal AZ, Kizer JR (2008) Cardiogenic and aortogenic brain embolism. *J Am Coll Cardiol* 51(11):1049–1059
- Ferro JM (2003) Cardioembolic stroke: an update. *Lancet Neurol* 2(3):177–188
- Paraskevaïdis IA, Michalakeas CA, Papadopoulos CH, Anastasiou-Nana M (2011) Cardiac tumors. *ISRN Oncol* 2011:208929
- Sparrow PJ, Kurian JB, Jones TR, Sivananthan MU (2005) MR imaging of cardiac tumors. *Radiographics* 25(5):1255–1276
- Bogaert J, Dymarkowski S, Taylor AM (2005) Clinical cardiac MRI. Springer, Berlin Heidelberg New York
- Kim EY, Choe YH, Sung K, Park SW, Kim JH, Ko YH (2009) Multidetector CT and MR imaging of cardiac tumors. *Korean J Radiol* 10(2):164–175
- Karcaaltincaba M, Aktas A (2011) Dual-energy CT revisited with multidetector CT: review of principles and clinical applications. *Diagn Interv Radiol* 17(3):181–194
- Johnson TR, Krauss B, Sedlmair M, Grasruck M, Bruder H, Morhard D, Fink C, Weckbach S, Lenhard M, Schmidt B, Flohr T, Reiser MF, Becker CR (2007) Material differentiation by dual energy CT: initial experience. *Eur Radiol* 17(6):1510–1517
- Kang MJ, Park CM, Lee CH, Goo JM, Lee HJ (2010) Dual-energy CT: clinical applications in various pulmonary diseases. *Radiographics* 30(3):685–698
- Hur J, Kim YJ, Lee HJ, Nam JE, Ha JW, Heo JH, Chang HJ, Kim HS, Hong YJ, Kim HY, Choe KO, Choi BW (2011) Dual-enhanced cardiac CT for detection of left atrial appendage thrombus in patients with stroke: a prospective comparison study with transesophageal echocardiography. *Stroke* 42(9):2471–2477
- Hur J, Kim YJ, Lee HJ, Nam JE, Hong YJ, Kim HY, Lee JW, Choi BW (2012) Cardioembolic stroke: dual-energy cardiac CT for differentiation of left atrial appendage thrombus and circulatory stasis. *Radiology* 263(3):688–695
- Gomes AS, Lois JF, Child JS, Brown K, Batra P (1987) Cardiac tumors and thrombus: evaluation with MR imaging. *AJR Am J Roentgenol* 149(5):895–899
- Weinsaft JW, Kim HW, Shah DJ, Klem I, Crowley AL, Brosnan R, James OG, Patel MR, Heitner J, Parker M, Velazquez EJ,

- Steenbergen C, Judd RM, Kim RJ (2008) Detection of left ventricular thrombus by delayed-enhancement cardiovascular magnetic resonance prevalence and markers in patients with systolic dysfunction. *J Am Coll Cardiol* 52(2):148–157
17. Weinsaft JW, Kim RJ, Ross M, Krauser D, Manoushagian S, LaBounty TM, Cham MD, Min JK, Healy K, Wang Y, Parker M, Roman MJ, Devereux RB (2009) Contrast-enhanced anatomic imaging as compared to contrast-enhanced tissue characterization for detection of left ventricular thrombus. *JACC Cardiovasc Imaging* 2(8):969–979
  18. Paydarfar D, Krieger D, Dib N, Blair RH, Pastore JO, Stetz JJ Jr, Symes JF (2001) In vivo magnetic resonance imaging and surgical histopathology of intracardiac masses: distinct features of subacute thrombi. *Cardiology* 95(1):40–47
  19. Grebenc ML, Rosado de Christenson ML, Burke AP, Green CE, Galvin JR (2000) Primary cardiac and pericardial neoplasms: radiologic-pathologic correlation. *Radiographics* 20(4):1073–1103; quiz 1110–1071, 1112
  20. Scheffel H, Baumüller S, Stolzmann P, Leschka S, Plass A, Alkadhi H, Schertler T (2009) Atrial myxomas and thrombi: comparison of imaging features on CT. *AJR Am J Roentgenol* 192(3):639–645
  21. Claussen C, Kohler D, Scharl M, Felix R (1983) Computer tomographic and echocardiographic diagnosis of intracardial space occupying masses. *Rofo* 138(3):296–301
  22. Taylor AJ, Cerqueira M, Hodgson JM, Mark D, Min J, O’Gara P, Rubin GD, American College of Cardiology Foundation Appropriate Use Criteria Task F, Society of Cardiovascular Computed T, American College of R, American Heart A, American Society of E, American Society of Nuclear C, North American Society for Cardiovascular I, Society for Cardiovascular A, Interventions, Society for Cardiovascular Magnetic R, Kramer CM, Berman D, Brown A, Chaudhry FA, Cury RC, Desai MY, Einstein AJ, Gomes AS, Harrington R, Hoffmann U, Khare R, Lesser J, McGann C, Rosenberg A, Schwartz R, Shelton M, Smetana GW, Smith SC, Jr. (2010) ACCF/SCCT/ACR/AHA/AASE/ASNC/NASCI/SCAI/SCMR 2010 appropriate use criteria for cardiac computed tomography. a report of the American College of Cardiology Foundation Appropriate Use Criteria Task Force, the Society of Cardiovascular Computed Tomography, the American College of Radiology, the American Heart Association, the American Society of Echocardiography, the American Society of Nuclear Cardiology, the North American Society for Cardiovascular Imaging, the Society for Cardiovascular Angiography and Interventions, and the Society for Cardiovascular Magnetic Resonance. *J Am Coll Cardiol* 56(22):1864–1894
  23. AscI CCT, Group CMRGW, Tsai IC, Choi BW, Chan C, Jinzaki M, Kitagawa K, Yong HS, Yu W, Asian Society of Cardiovascular Imaging Cardiac Computer T, Cardiac Magnetic Resonance Imaging Guideline Working G (2010) ASCI 2010 appropriateness criteria for cardiac computed tomography: a report of the Asian society of cardiovascular imaging cardiac computed tomography and cardiac magnetic resonance imaging guideline working group. *Int J Cardiovasc Imaging* 26(Suppl 1):1–15